Short communication

Ex situ study of chloride contamination on carbon supported Pt catalyst

Alfred Lam [a,b], Hui Li [b,*], Shengsheng Zhang [b], Haijiang Wang [b,**], David P. Wilkinson [a,b], Silvia Wessel [c], Tommy T.H. Cheng [c]

[a] Chemical & Biological Engineering and Clean Energy Research Centre – University of British Columbia, 2360 East Mall, Vancouver, BC, Canada V6T 1Z3
[b] National Research Council of Canada – 4250 Wesbrook Mall, Institute for Fuel Cell Innovation, Vancouver, BC, Canada V6T 1W5
[c] Ballard Power Systems, Inc., 9000 Glenlyon Parkway, Burnaby, BC, Canada V5J 5J8

ARTICLE INFO

ABSTRACT

The effect of ppm levels of chloride ions on a carbon supported platinum catalyst was examined using an ex situ electrochemical quartz crystal microbalance (EQCM) method. The dissolution of Pt as chloride complexes and the adsorption of chloride ions resulted in a loss of electrochemical surface area (ECSA) by 4%, 7% and 13% for the respective chloride concentrations of 500 ppm, 1000 ppm and 2000 ppm. Catalyst durability was examined by cyclic voltammetry (CV) and scanning electron microscopy (SEM) in the presence of 1000 ppm chloride. The beginning of life (BOL) ECSA of $8.1\,cm^2\,cm^{-2}$ was significantly reduced to an end of life (EOL) ECSA of $3.2\,cm^2\,cm^{-2}$ after cycling in the presence of 1000 ppm chloride.

Crown Copyright © 2012 Published by Elsevier B.V. All rights reserved.

1. Introduction

Hydrogen based polymer electrolyte membrane (PEM) fuel cells are attractive for a wide range of applications (e.g., stationary, transportation) due to its high efficiency and zero emissions. Significant technological advancements have been made towards its large scale deployment in various market applications, but challenges with the cost, reliability and durability of fuel cell components still remain.

Since sources of hydrogen are not found naturally, they must be derived from the reforming of conventional fuels (e.g., natural gas, methanol etc.) [1], renewably through solar or wind powered electrolysis [2], alternatively from waste hydrogen generated from chemical plants, or other methods. The quality and contamination species that affect fuel cell performance will differ with the type of the H_2 generation method. The focus of this work is on H_2 as a feed stream for PEM fuel cells generated as by-product from the production of HCl during the electrochemical generation of chlorine gas [3] that can contain ppm levels of chlorine which will have a detrimental effect on the fuel cell performance and durability.

Recent studies of in situ chloride contamination have shown a significant drop in fuel cell performance and durability [3–6] when ppm levels HCl or NaCl solution is injected into the fuel stream [3] and/or the air stream [3–6]. This was attributed to a cathodic increase in mass transfer and charge transfer resistances [3] and a reduced ECSA arising from the blocking of platinum sites by chloride adsorption and platinum dissolution. Similar contamination mechanisms were also reported from ex situ experiments, primarily focused on the use of flat platinum metal electrodes, using a rotating ring-disk electrode (RRDE) [7] and EQCM [8,9] combined with ICP-mass analysis [9].

In this paper, an ex situ examination of a carbon supported platinum catalyst (Pt/C) is conducted using an EQCM method [10] as a complementary technique to our in situ study of chloride contamination [3] in order to provide better mechanistic understanding of the chloride contamination mechanisms in real fuel cell systems.

2. Materials and methods

2.1. Solution preparation

A 25-mL solution was prepared with sulfuric acid (ACS Fisher Scientific) and 18.2 MΩ deionized (DI) water to a concentration of 0.5 M H_2SO_4. Prior to each experiment, the solution was deaerated by bubbling nitrogen gas. The chloride concentrations of 500 ppm, 1000 ppm, and 2000 ppm were prepared by a successive addition of 1 M hydrochloric acid (ACS Fisher Scientific) to the 0.5 M H_2SO_4 solution during experimentation.

* Corresponding author. Tel.: +1 604 221 3000.
** Corresponding author. Tel.: +1 604 221 3038.
E-mail addresses: hui.li@nrc.gc.ca (H. Li), haijiang.wang@nrc.gc.ca (H. Wang).
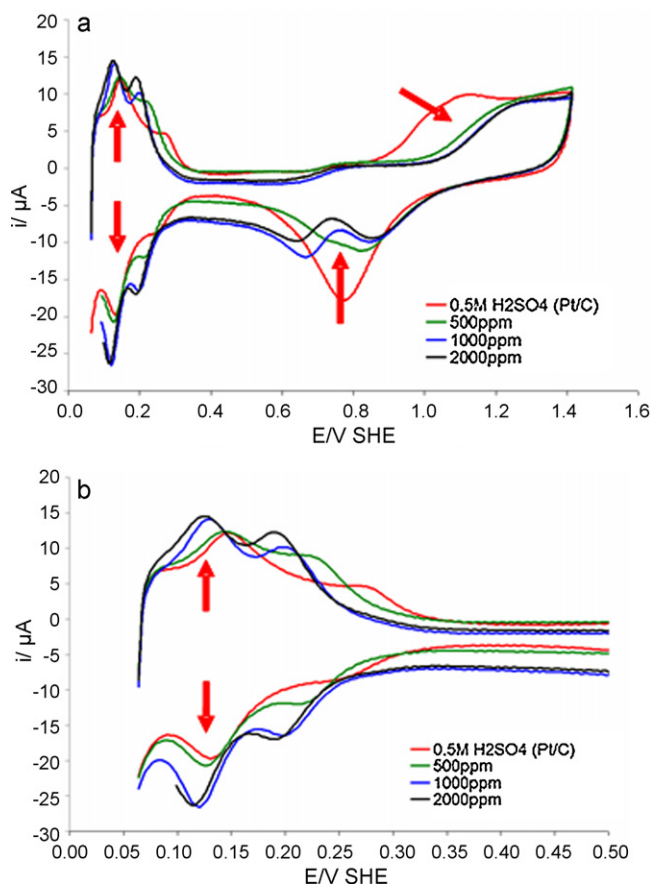
Fig. 1. (a) CVs (scan rate = 40 mV s^{-1}) for a bare Pt resonator in 0.5 M H$_2$SO$_4$ with the successive addition of chloride and (b) hydrogen adsorption/desorption region.

Fig. 2. (a) CVs (scan rate = 40 mV s^{-1}) for a resonator with a loading of 40 μg Pt cm^{-2} in 0.5 M H$_2$SO$_4$ with the successive addition of chloride and (b) hydrogen adsorption/desorption region.

2.2. Catalyst ink preparation

A catalyst ink was prepared by combining 46 wt% Pt/C catalyst (TKK – Tanaka Kikinzoku Kogyo), a 5% Nafion® solution, ethanol and 18.2 MΩ DI water. The ink solution was deposited onto 0.196 cm^2 standard finished 9 MHz AT cut Pt quartz resonators (Princeton Applied Research Inc.) to yield a loading of 40 μg Pt cm^{-2} and 20 μg Pt cm^{-2} for the respective short term (i.e., 50–85 cycles per chloride concentration) and durability (i.e., 1000 cycles) testing. The Pt resonators were pre-treated before the catalyst ink deposition by: (a) rinsing in 18.2 MΩ DI water, (b) dipping into a solution of 1:1 volume of H$_2$SO$_4$ and 30 wt% H$_2$O$_2$ for 30 s [11], (c) rinsing in 18.2 MΩ DI water.

2.3. Quartz crystal microbalance (QCM) and CV experiments

QCM and CV experiments were carried out at ambient conditions (25 °C, 1 atm) with a QCA922 Quartz Crystal Microbalance (Seiko, Princeton Applied Research) and a PARSTAT 2263 potentiostat (Princeton Applied Research) in a three-electrode glass cell arrangement that includes a Pt quartz resonator working electrode, a Pt rod counter electrode and a Hg/HgSO$_4$ reference electrode (Sentek). A pre-treatment procedure from the previous section was used for the Pt quartz resonator working electrode. For the presentation of the results, all electrode potentials are referenced to the standard hydrogen electrode (SHE).

For the bare platinum resonator samples, CV scans were carried out between 0.05 V and 1.40 V vs. SHE at a scan rate of 40 mV s^{-1}. For the Pt/C samples, CV scans were carried out between 0.05 V and 1.20 V vs. SHE, to avoid carbon corrosion. A scan rate of 40 mV s^{-1}
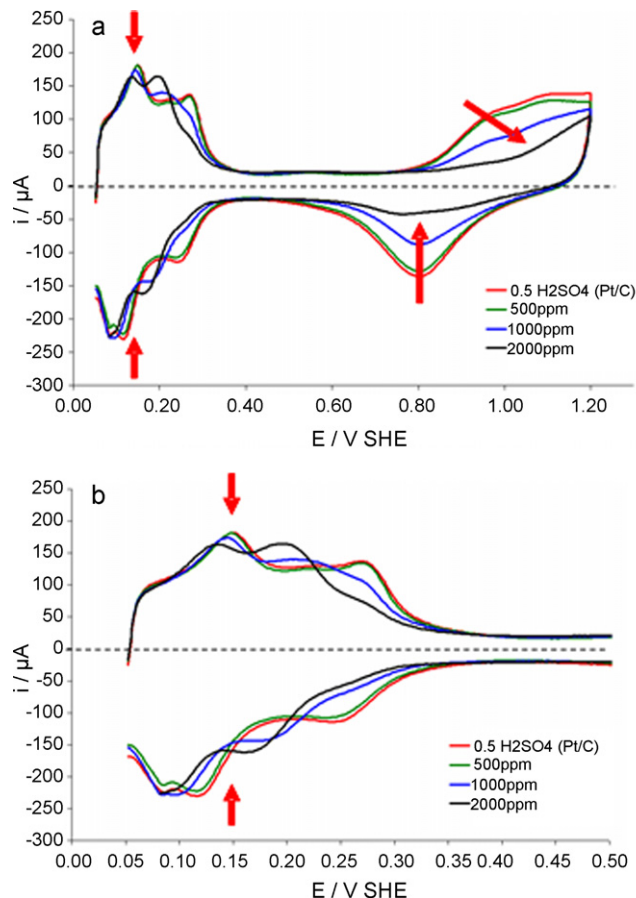
and 50 mV s^{-1} were used for short term and durability testing respectively.

The change in frequency was recorded over the CV sweep and is proportional to the mass change as shown in Eq. (1).

$$\Delta m = -\frac{\Delta f}{C_f} \tag{1}$$

where Δm = mass change per unit area; $\Delta f = f(E)$ = change in resonant frequency (Hz); and C_f = Sauerbrey constant.

The Sauerbrey constant was determined by a Cu underpotential deposition method [11]. This involved a deposition of Cu on the Pt/C resonator samples followed by an anodic stripping of the Cu. The Sauerbrey constant C_f for the Pt/C resonator was experimentally determined to be 1861 Hz cm^2 μg^{-1}.

3. Results and discussion

The CVs for a bare platinum resonator with increasing chloride concentration is shown in Fig. 1a and can be segmented into three regions: (i) hydrogen adsorption/desorption region (0.05–0.4 V); (ii) double layer region (0.40–0.75 V); and (iii) Pt oxide region (0.75–1.40 V).

The hydrogen adsorption/desorption region in Fig. 1b exhibited a similar "squeezing" effect, that was reported by Zolfaghari et al. [9], where there is a narrowing increase of the region due to a competitive co-adsorption between Cl$^-$ ions and hydrogen. A widening of the double layer region is suggested to be caused by the presence of Cl$^-$ ions at the platinum electrolyte interface [3]. In the
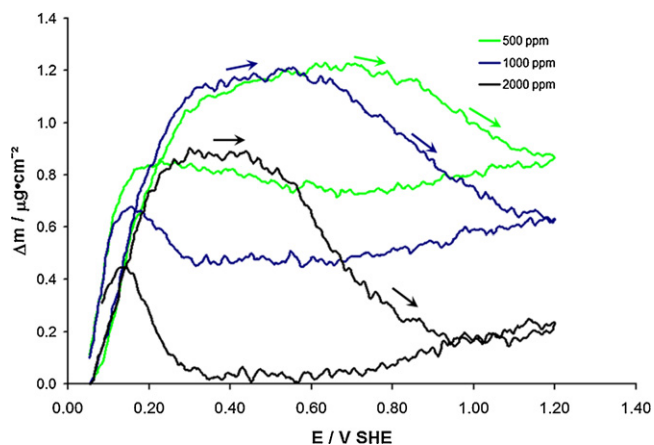
Fig. 3. Mass change for a resonator with 40 μg Pt cm^{-2} in 0.5 M H$_2$SO$_4$ with chloride concentrations of 500 ppm, 1000 ppm and 2000 ppm (scan rate = 40 mV s^{-1}).

oxide region, the chloride has delayed the formation of Pt oxide to a potential greater than 1.0 V and has decreased the reduction peak.

The CVs for a resonator with a loading of 40 μg Pt cm^{-2} with increasing chloride concentration are shown in Fig. 2a. The hydrogen adsorption/desorption region (Fig. 2b) for the supported catalyst showed a narrowing potential range and a decreased current instead of a narrowing potential range and an increased current as observed with the bare resonator. This is in agreement with the in situ CV testing on a carbon supported catalyst in a 50-cm^2 PEM fuel cell that we reported previously [3].
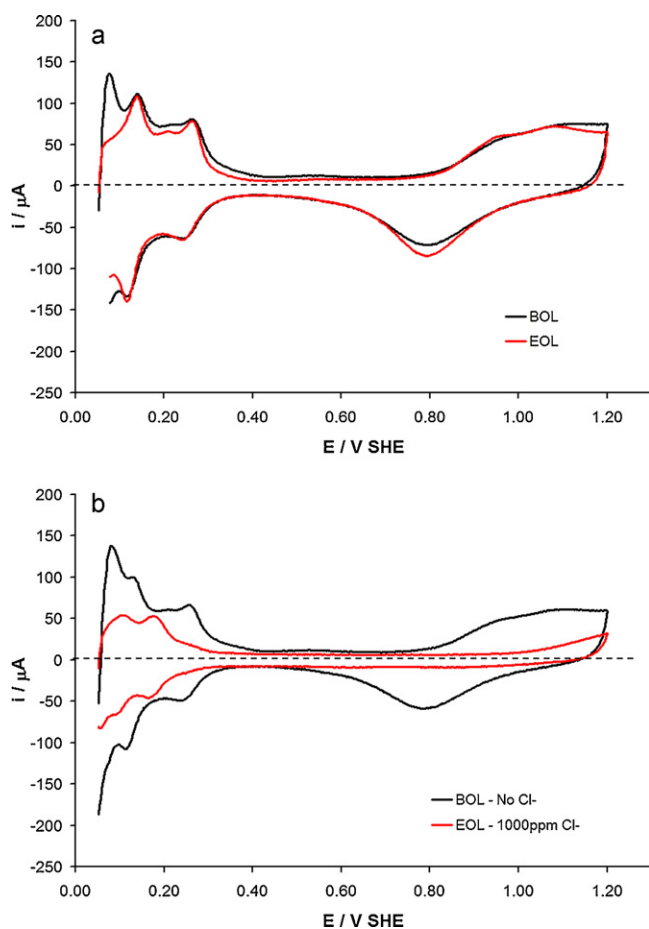

Fig. 4. BOL and EOL CVs (scan rate = 50 mV s^{-1}) for a resonator with a loading of 20 μg Pt cm^{-2} in 0.5 M H$_2$SO$_4$ – (a) without chloride and (b) with 1000 ppm chloride.

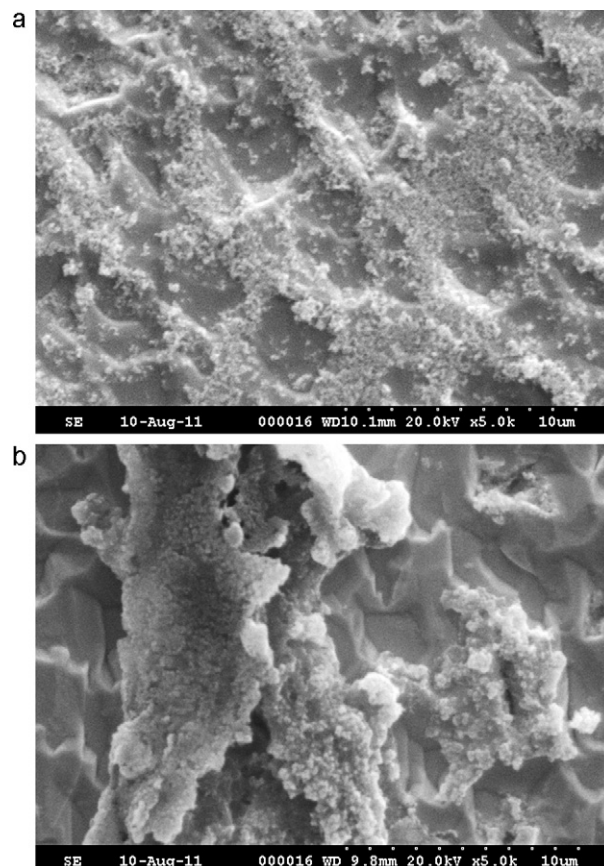**Fig. 5.** SEM of resonator with a loading of 20 μg Pt cm^{-2} in 0.5 M H$_2$SO$_4$ – (a) BOL without chloride and (b) EOL with 1000 ppm chloride.

Similar to the bare platinum resonators, there was a strong suppression of Pt/PtO peaks. In the forward scan, the oxide formation is significantly delayed by the adsorbed Cl$^-$ ions and conversely on the backward scan, there was a decreased reduction peak. Yadav et al. [8] has attributed this to the dissolution of Pt by the formation of the soluble chloride complexes shown in Eqs. (2) and (3).

$$Pt + 4Cl^- \rightarrow PtCl_4{}^{2-} + 2e^- \tag{2}$$

$$Pt + 6Cl^- \rightarrow PtCl_6{}^{2-} + 4e^- \tag{3}$$

This loss of mass due to dissolution is shown in the mass response in Fig. 3. In the forward scan, the dissolution kinetics can be qualitatively correlated to the difference in slope. At higher concentrations of chloride, the loss of mass increases as exemplified by the steeper slopes. In this range there is a competitive mechanism of Pt dissolution and oxide formation. Furthermore, there is an earlier onset of this loss at higher concentrations (i.e., ~0.75 V for 500 ppm, 0.6 V for 1000 ppm and 0.55 V for 2000 ppm) beyond the plateau region.

The mechanisms of Pt dissolution accelerated by chloride adsorption have resulted in a loss in ECSA. The ECSA was determined to be reduced by 4%, 7%, and 13% for the respective chloride concentrations from 500 ppm to 2000 ppm in comparison with the ECSA with 0 ppm HCl.

The ex situ durability of 20 μg Pt cm^{-2} was examined with and without the addition of chloride. CVs for two different resonator samples at BOL and at EOL (i.e., after 1000 scans) are shown in Fig. 4. It was clearly shown that cycling has little effect on the ECSA in the absence of chloride (Fig. 4a) as determined by the BOL and EOL ECSA for of 7.1 cm^2 cm^{-2} and 6.9 cm^2 cm^{-2}, respectively. In the presence of 1000 ppm chloride (Fig. 4b), the ECSA was significantly

reduced to 3.2 cm^2 cm^{-2} at EOL. This effect is in agreement with our in situ fuel cell durability studies [3].

SEM images of a 20 μg Pt cm^{-2} resonator at BOL without chloride and at EOL with 1000 ppm chloride are shown in Fig. 5. Prior to the accelerated durability testing, smaller individual catalyst clusters can be seen (Fig. 5a) over the resonator surface. After 1000 CV cycles, the catalyst morphology appears to have changed into larger surface clusters (Fig. 5b) resulting in a loss of ECSA.

4. Conclusions

The effect of ppm levels of chloride ions on a carbon Pt/C was examined using an ex situ EQCM method. CVs for the resonator with a 40 μg Pt cm^{-2} loading had similar characteristics to the bare platinum resonator in the oxide region where the Pt/PtO peaks were suppressed due to the presence of chloride ions. However, in the hydrogen adsorption/desorption region the peaks did not have the characteristic squeezing and extending effect, instead the peaks narrowed and contracted. Compared to the ECSA at 0 ppm chloride, respective ECSA losses of 4%, 7%, and 13%, attributed to Pt dissolution and chloride adsorption, were observed in the presence of 500 ppm, 1000 ppm, and 2000 ppm chloride ions.

The durability of a 20 μg Pt cm^{-2} resonator sample was examined before and after 1000 CV cycles. After 1000 CV cycles in the presence of 1000 ppm Cl$^-$ ion, the ECSA was reduced by 60%.

Compared to BOL, the EOL SEM images show the presence of large particles on the catalyst surface.

References

[1] A.F. Ghenciu, Solid State Mater. Sci. 6 (5) (2002) 389–399.
[2] T. Abbasi, S.A. Abbasi, Renew. Sustain. Energy Rev. 15 (6) (2011) 3034–3040.
[3] H. Li, H. Wang, W. Qian, S. Zhang, S. Wessel, T.T.H. Cheng, J. Shen, S. Wu, Power Sources J. 196 (2011) 6249–6255.
[4] W. Yan, H. Chu, Y. Liu, F. Chen, J. Jang, Int. J. Hydrogen Energy 36 (9) (2011) 5435–5441.
[5] K. Matsuoka, S. Sakamoto, K. Nakato, A. Hamada, Y. Itoh, Power Sources J. 179 (2) (2008) 560–565.
[6] S. Ali, Q. Li, C. Pan, J.O. Jensen, L.P. Nielsen, P. Moller, Int. J. Hydrogen Energy 36 (2) (2011) 1628–1636.
[7] T.J. Schmidt, U.A. Paulus, H.A. Gasteiger, R.J. Behm, J. Electroanal. Chem. 508 (1–2) (2001) 41–47.
[8] A.P. Yadav, A. Nishikata, T. Tsuru, Electrochim. Acta 52 (26) (2007) 7444–7452.
[9] A. Zolfaghari, B.E. Conway, G. Jerkiewicz, Electrochim. Acta 47 (8) (2002) 1173–1187.
[10] J.M.D. Rodriguez, J.A.H. Melian, J.P. Pena, J. Chem. Ed. 77 (9) (2000) 1195–1197.
[11] V.W.S. Lam, D.C.W. Kannangara, A. Alfantzi, E.L. Gyenge, J. Phys. Chem. C 115 (6) (2011) 2727–2737.